DAS dataset analysis for reflection imaging with ambient noise in urban areas: Granada, Spain.

Introduction

Distributed Acoustic Sensing (DAS) is a relatively new technology. It has shown a great potential to improve seismic measurements that require dense spatial sensor coverage and a wide frequency range recording (Spica et al., 2020). DAS is based on optical time-domain laser reflectometry to measure strain or strain rate along an optical fiber. In practice, the resulting waveform is the average axial strain along a subset of the fiber optic cable (i.e., the gauge length). The main advantages of this technique are the high-density sensor coverage (only limited by the gauge length); that the sensing elements are insensitive to electrical noise, and the broadband nature of the DAS sensor. However, because DAS measures a tensor component (axial strain along the fiber), the measurements suffer from a stronger angular sensitivity than standard seismometers. DAS also typically has a lower signal-to-noise ratio than standard seismometers, although this is rapidly changing with advances in both cable and interrogator design. Its use for subsurface characterization in urban areas is still in its infancy (Spica et al., 2020). In this work, we present the results using autocorrelation of ambient noise recorded during one day using a fiber-optic telecom cable in the city of Granada (Spain).

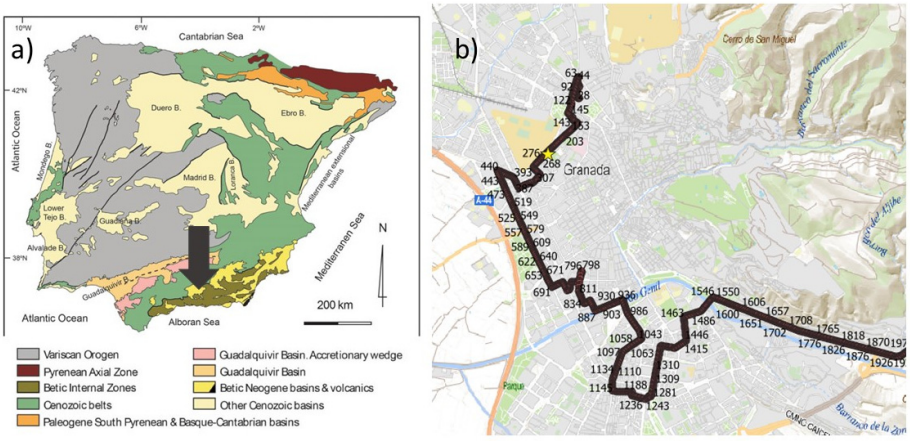

Figure1. *a) Location of the city of Granada on Iberian Peninsula geological map (from Braga and Cunha, 2019) b) Location of underground fiber-optic cable in the city of Granada with channel numbering. The yellow star marks the location of the three-component seismic station.*

Geological setting

Granada city is located in the Granada Basin south of the Iberian Peninsula (Figure1a). This largest Neogene-Quaternary intramontane basin of the Betic Cordillera occurs between the External and Internal Zones, the two main domains of the cordillera. The basement of the basin in the Granada city area consists of metamorphic rocks (Alpujarride complex) of the Internal Zones. Active deformation with an associated moderate level of seismicity are recorded. This deformation is controlled by a NNW-SSE compressive regime and a near orthogonal extensive regime (Sanz de Galdeano et al., 2012).Three depositional sequences can be considered: Upper Miocene marine sediments, Upper Miocene continental sediments, and Pliocene to Quaternary sediments. The seismic unconformities of these three sequences can be distinguished in the legacy seismic reflection profiles acquired along the basin as prominent reflectors (Morales et al., 1990; Rodríguez-Fernández and Sanz de Galdeano, 2006). This geological setting can be critical for strong amplification effects in case of ground motion.

Dataset

The fiber-optic cable is used for communicating the radio-telescope of IRAM (Institute of Radioastronomie Millimetrique) in Sierra Nevada with its headquarters in Granada city. Figure 1b shows the location of a sector of this cable in the city of Granada. The DAS interrogator was Febus-

Optics A1-R, and strain rate datasets were acquired along 4167 channels during a one-day experiment. The frequency rate was 2000 Hz. One-hour files were stored in HDF5 format with 3001 blocks of 1 s record length. Each file has a total size of 240 Gb. We will focus on channels 201 to 300, which are the closest to the 3C station (yellow star in Figure 1b). The station consisted of a Lennartz 5 s 3C sensor connected to a Centaur datalogger.

Methodology

In this work, we will apply the autocorrelation technique to retrieve the reflectivity response of the subsurface (Romero and Schimmel, 2018). This information is critical to build 3D geological models suitable for any infrastructure planning in populated areas. The workflow included converting datasets by channel in SAC format, keeping the original data sampling from ten HDF5 files (10 hours). This has been done with a Python script. Next, autocorrelations were obtained for a 300s time window, overlapped by 150 s after filtering the signal between 5 to 30 Hz. This range has been chosen supported by the amplitude spectra (Figures 2b and 4b). The maximum lag was 10 s. The algorithm for autocorrelation was introduced by Schimmel (1999). We have built a Python script that included the function ppc2_method.py programmed by Bonilla and Ben-Zion (2021). The last step was to stack all the autocorrelations corresponding to each channel using the time-frequency domain phase weighted stack (tf-PWS) (Schimmel and Gallart, 2007). The same procedure has been used for the 3C seismic station dataset. We have used Seismic Unix open software (https://wiki.seismic-unix.org/doku.php) for displaying the reflection dataset. In addition, we have applied the H/V microtremor technique to this latter dataset for further interpretation using the Geopsy package (www.geopsy.org).

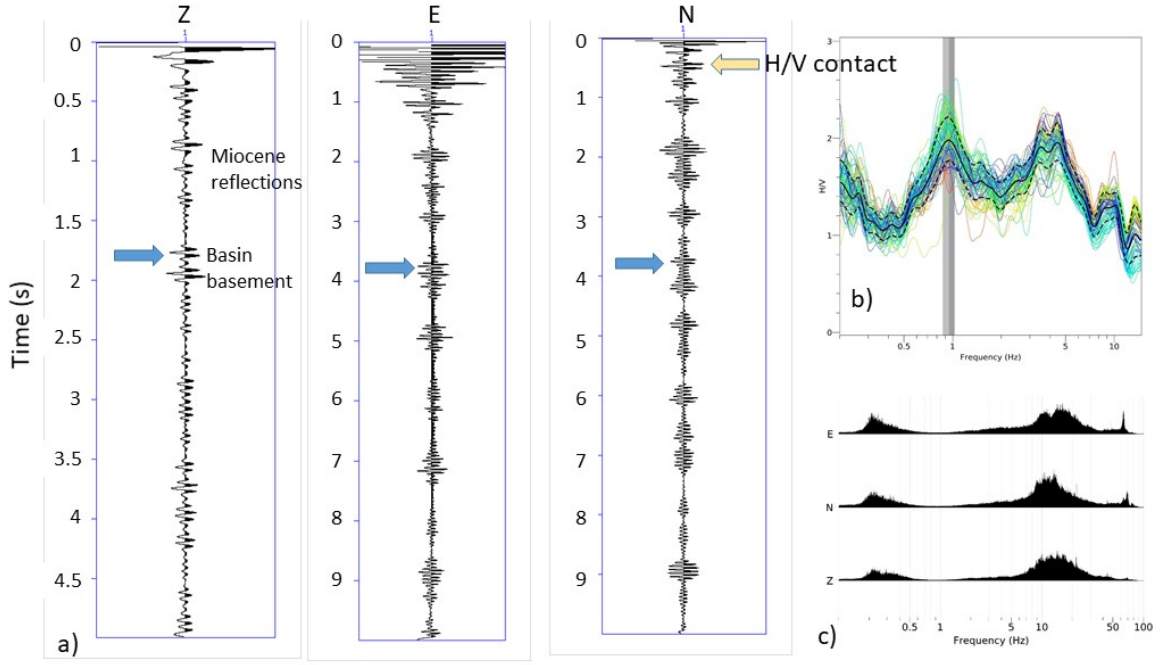

Figure 2. *a) Autocorrelation results for the 3C record at the seismic station located close channels 257 and 258 of the fiber-optic cable b) H/V plot from the same record c) amplitude spectra of the three components. Blue arrows mark reflections that may be related to the basin basement. The yellow arrow marks the reflection possibly associated with a major shallow acoustic impedance detected in the H/V plot.*

Results

Figure 2a shows the autocorrelation stacks of the three components of the seismic station. We focus first on the vertical component since it can be directly related to active seismic results. Several significant amplitude changes can be distinguished: at 0.8, 1.03, 1.3, 1.73, and 1.9 s two-way time (TWT). As introduced in the geological setting, main reflectors may correspond to contacts within the Miocene sediments. High amplitude and correlation with identified reflection in active seismic datasets in the vicinity of Granada suggest that the 1.9s TWT may be related to the sediments/basement contact.

Autocorrelation stacks corresponding to the North and East components show a coherent response among them. Vp/Vs ratios from literature raises the possibility that the reflection package for horizontal components around 4 s being the reflection from the basin basement. Earlier reflections should be related to acoustic impedance contrasts within the Miocene to Pliocene sequences. H/V result is also displayed from 0.2- 15 Hz (Figure 2b). We have fixed the lower end of the frequency range considering the natural frequency of the seismic sensor. There is a good correlation between the reflection observed at 0.53 s in the North component (Figure 2a) and the frequency corresponding to the maximum in the H/V plot. This frequency can be transformed into TWT of shear-wave reflections using a simple relationship TWT=$T_{H/V}$/2 where $T_{H/V}$ is the period corresponding to a maximum of the H/V plot. The frequency 0.94 Hz can be related to a TWT of 0.53 s. Horizontal reflectivity obtained from the seismic station can be compared with DAS autocorrelations since this technique records seismic waves in that component along the fiber. Although we do not convert the DAS strain rate into velocity for complete calibration, a comparison can be performed since the obtained waveform matches the ones derived from standard seismic sensors in both frequency and phase characteristics (Jousset et al., 2018).

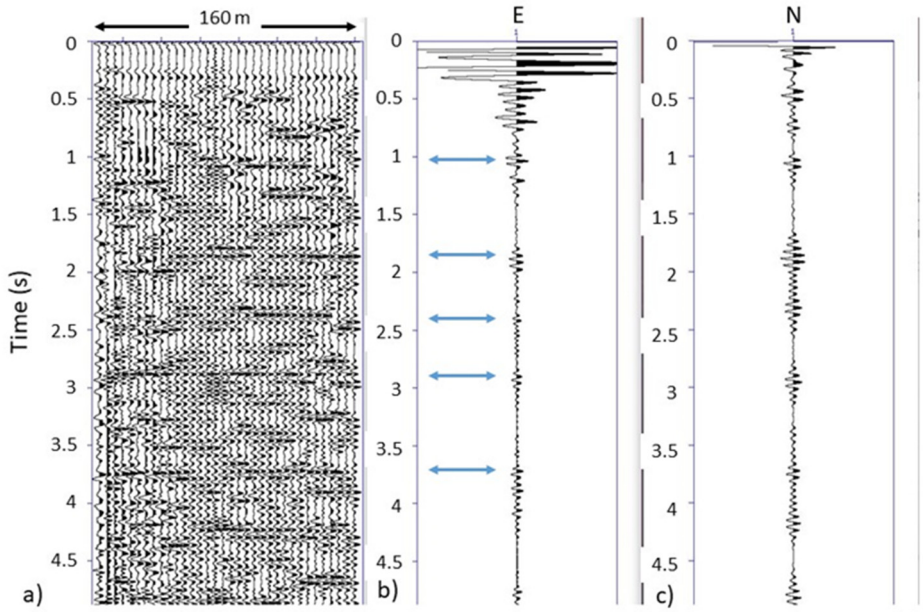

Figure 3. *a) Autocorrelation stacks obtained for channels 267 to 300 of the DAS array b) and c) autocorrelation stacks for E and N components of the 3C seismic station. Blue arrows mark significant amplitude changes observed in both experiments.*

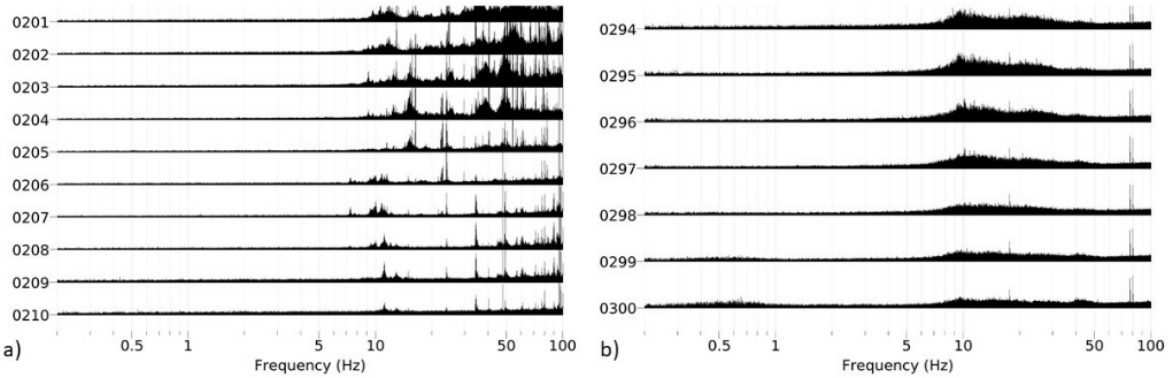

Figure 4. *a) Amplitude spectra for channels 201 to 210 with no clear reflectivity response from autocorrelation and b) for channels 294 to 300 with appropriate ambient noise energy for the autocorrelation technique.*

Strain rate records for DAS channels 200 to 300 have been analyzed following the autocorrelation procedure explained in the previous section. Figure 3a displays the autocorrelation stacks of 10 hours records for channels 267 to 300. This group presents the best consistency with the results from the seismic station. Some of the observed amplitude changes correspond to the ones obtained with the 3C sensor. The rest of the autocorrelations for the channel range studied do not produce a clear result. The absence of useful energy can be related to the fiber-optic cable's lack of optimum ground coupling.

Noise characteristics should be similar to the whole sector, considering it corresponds to a location along the same street (Figure 1b). Figure 4a shows the amplitude spectra for a segment with incoherent results where several anomalous maxima. The amplitude spectra for a sector with useful energy and good signal autocorrelations are displayed in Figure 4b. The use of amplitude spectra can be a tool for selecting channels with appropriate ambient noise energy for the autocorrelation procedure.

Conclusions

DAS technique has the advantage that may record data from numerous seismic sensors along existing underground cables, instead of using traditional seismic instrumentation and more punctual deployments in the city. Additionally, passive seismic techniques do not imply the use of any active sources, reducing the logistical complexity of the surveys. Identifying regions with appropriate ambient noise energy should be a first step for retrieving subsurface information from DAS datasets. Amplitude spectra calculation could be a tool for selecting records with useful energy. This work highlights the usefulness of recording strain rate along urban fiber-optic cables and the use of ambient noise techniques such as autocorrelation. The retrieved reflectivity information can be used to complete 3D geological models, which are essential for urban development projects, where the density of channels warrants a high spatial resolution.

Acknowledgments

We are grateful to IRAM in Granada and IGN for letting us to use their installations and optic fiber to acquire the data, we thank specially Miguel A. Muñoz for all the information and help provided. We thank *Casa Madre de las Misioneras del Santísimo Sacramento* in Granada for allowing us to install the 3C seismometer in their dependencies and Maria Galán from IGN to manage the seismometer location. This research was supported by National Science Foundation Grant EAR-2022716 to Z. Spica. MS thanks SANIMS (RTI2018-095594-B-I00).

References

Bonilla, L.F., Ben-Zion, Y., [2021]. Detailed space–time variations of the seismic response of the shallow crust to small earthquakes from analysis of dense array data, *Geophysical Journal International*, 225, 298–310.

Braga, J.C. & Cunha, P.P. [2019] Introduction in *The Geology of Iberia: A Geodynamic Approach*. C. Quesada and J. T. Oliveira (eds.), Regional Geology Reviews. Springer, Cham.

Jousset, P., Reinsch, T., Ryberg, T., Blanck, H., Clarke, A., Aghayev, R., Hersir, G.P., Henninges, J., Weber, M. & Krawczyk, C. M. [2018]. Dynamic strain determination using fibre-optic cables allows imaging of seismological and structural features. *Nature Communications*, 9(1), 1-11.

Morales, J., Vidal, F., De Miguel, F., Alguacil, G., Posadas, A. M., Ibáñez, J. M., Guzmán, A. & Guirao, J. M. [1990]. Basement structure of the Granada basin, Betic Cordilleras, southern Spain. *Tectonophysics*, 177(4), 337-348.

Rodríguez-Fernández, J., & De Galdeano, C. S. [2006]. Late orogenic intramontane basin development: the Granada basin, Betics (southern Spain). *Basin Research*, 18(1), 85-102.

Romero, P., & Schimmel, M. [2018]. Mapping the basement of the Ebro Basin in Spain with seismic ambient noise autocorrelations. Journal of Geophysical Research: *Solid Earth*, 123, 5052–5067.

Sanz de Galdeano, C., García Tortosa, F. J., Peláez Montilla, J. A., Alfaro García, P., Azañón, J. M., Galindo Zaldívar, J., López Casado, C., López-Garrido, A.C., Rodríguez-Fernández, J. & Ruano, P. [2012]. Main active faults in the Granada and Guadix-Baza basins (Betic Cordillera). *Journal of Iberian Geology* 38 (1), 209-223.

Schimmel M., [1999], Phase cross-correlations: design, comparisons and applications, *Bull. Seismol. Soc. Am.,* 89, 1366-1378

Schimmel, M., & Gallart, J. [2007]. Frequency-dependent phase coherence for noise suppression in seismic array data. *Journal of Geophysical Research*, 112, B04303. https://doi.org/10.1029/2006JB004680.

Spica, Z. J., Perton, M., Martin, E. R., Beroza, G. C., & Biondi, B. [2020]. Urban seismic site characterization by fiber-optic seismology. Journal of Geophysical Research: *Solid Earth*, 125(3), e2019JB018656.